Optical Tweezers for Precise Control of Micro-bubble Arrays: In Situ Temperature Measurement

Tristan M. Burns, Daryl Preece, Timo A. Nieminen, Halina Rubinsztein-Dunlop

School of Mathematics and Physics, The University of Queensland, Brisbane, Queensland 4072 Australia

ABSTRACT

We use highly a focused laser beam incident on a carbon coated coverslip to create microcavitation. Full optical control of the radii of the bubbles is attained. Multiple bubbles can also be created and their size changed independently. The dynamics of such multi-bubble systems are studied. These bubble systems generate strong flows such as Marangoni convection and also large thermal gradients. Since the size of the micro-bubbles is highly dependent on the temperature, we anticipate that these systems can be used for precise temperature control of samples. These methods are of use when the knowledge of exact and local temperature profiles are of importance. Furthermore, since bubble expansion can generate orders of magnitude more force than conventional optical tweezers, systems have application in manipulation of particles where large forces are required. We present methods based on optical tweezers for using the generated bubbles as thermal sensors and as opto-mechanical transducers.

Keywords: Microcavitation, cavitation, optical tweezers, PID control, micromachines, in situ temperature measurement

1. INTRODUCTION

The manipulation of induced cavitation presents the possibility for novel actuation mechanisms for optomechanical devices. Cavitation is readily induced via chemical reactions, electrolysis and heating. Of particular interest here is laser induced cavitation, due to the relative ease of initiation and capacity for power modulation.
Though several examples of micro cavitation devices exist, a prominent commercial example being the ink-jet printer [1] where the rapid growth of vapour bubbles accelerate liquid though a nozzle forming a droplet for deposition onto paper. Precise control over laser induced bubbles has not yet been demonstrated.

Recent developments in the field have further demonstrated the applications of cavitation in microfluidic devices. Laser induced microcavitation has been demonstrated as a pump, through the exploitation of asymmetric currents surrounding bubbles pulsed in a cavity of appropriate geometry [2]. Similarly, on demand droplet fusion within microfluidic channels has been facilitated through the generation of explosively expanding cavitation [3]. Cavitation has successfully actuated rapid, consistent picolitre droplet generation in microfluidic channels [4]. Tuneable static and pulsatile chemical gradients have been achieved using acoustically activated bubbles arranged in a ladder like array [5]. The effects of Marangoni currents in optical tweezers generated microcavitation has been examined and identified to attract particles over greater distances, with greater forces than provided by optical trapping [6].

Microcavitation has also been demonstrated as a novel tool in the biological sciences. The generation of microcavitation from the absorption of laser radiation by located microparticles and nanoparticles has been demonstrated as a method for highly localised cell destruction [7], and this has been proposed as a dynamic mode for selective cancer treatment involving the overlapping of bubbles inside the cell volume [8]. Sonoporation, or sonically enhanced permeability of cell membranes, has been demonstrated using both laser

Optical Trapping and Optical Micromanipulation X, edited by Kishan Dholakia, Gabriel C. Spalding,
Proc. of SPIE Vol. 8810, 88102B · © 2013 SPIE · CCC code: 0277-786X/13/$18 · doi: 10.1117/12.2024254

and acoustically induced microcavitation [9]. Single cell lysis via shock waves caused by laser induced microcavitation, has facilitated single cell proteomics [10].

Developments in optical tweezers control also demonstrate the suitability of these setups as a tool for microcavitation generation and control. Closed loop control has been implemented to optical trapping, with SLM facilitated holographic feedback moving the trap in accordance with the trapped particles motion, resulting in a considerable increase in trap stiffness [11]. Holographic optical tweezers systems have provided accurate, multispot, x,y,z control, using intuitive interfaces such as the Apple iPad [12]. Furthermore, demonstrated advances in stereoscopic optical tracking of particles, with accuracies on the order of nanometres, provides an avenue for precision tracking of both probing particles and microcavitation radii [13]. Based on using 2D tracking of particles in each stereo image to provide 3D tracking of particles, this level of tracking accuracy allows for the correction of perturbations due to Brownian motion, via hologram feedback displayed on an Spatial Light Modulator (SLM) [13]. These control approaches can be readily applied and refined for microcavitation control in an optical tweezers setup.

While numerous applications of microcavitation have been presented, precise, sub-micron, variable control of microcavitation has remained a relatively undeveloped area of investigation. A flexible control, responsive to variations in power absorption and hence cavitation radius would be of benefit to many of the applications previously selected. The following work details the development of a Proportional Integral Derivative (PID) control system regulating laser induced microcavitation radii from 4-10 microns, with a standard deviation in the radius on the order of 20nm. Multiple bubble array control is demonstrated, and preliminary temperature measurements are estimated in the vicinity of the controlled cavitation.

2. EXPERIMENTAL SET-UP

2.1. Details of Induced Cavitation and Detection Systems

A custom optical tweezers microscope setup was constructed, to provide optical trapping and cavitation generation simultaneously. The setup consisted of an inverted microscope using a 100X objective, with LED illumination. Two near infrared (NIR) lasers were employed to enable the trapping of a probe particle for temperature measurement and cavitation generation and control respectively. A Ti-Sapphire Laser (Coherent Mira 900) at 780nmwas used to trap a probe particle during temperature measurement. A fiber laser at 1064nm (IPG Photonics YLD-5) provided the beam incident on the Holoeye HEO 1080p SLM, for cavitation generation and modulation. The Setup was imaged using a Prosilica GE680 camera. The setup is depicted in Fig. 1.
.

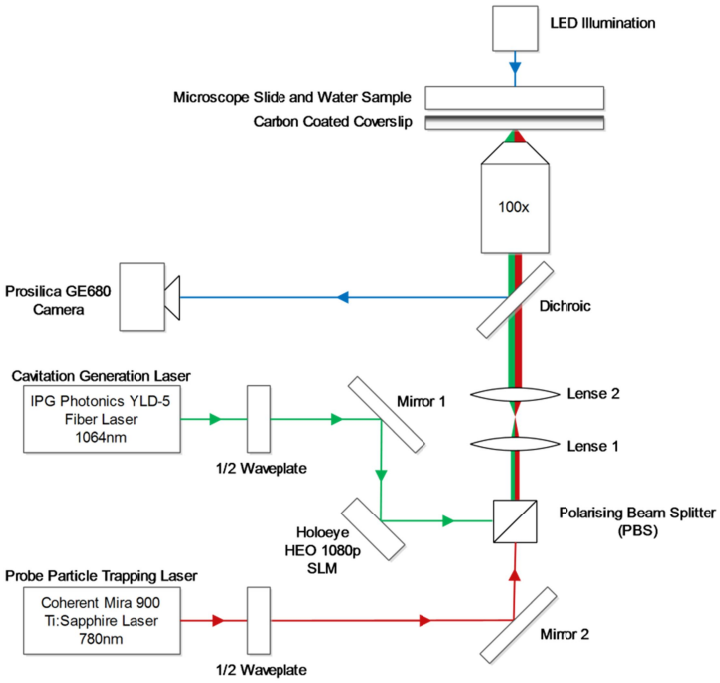

Fig. 1: Schematic of optical microcavitation and optical trapping set-up. The experimental set up uses two near infrared (NIR) lasers to accommodate cavitation generation and probing simultaneously.

2.2. Cover Slip Preparation

Glass cover slides (24mm × 50mm) with a thickness of 100 µm were cleaned in piranha solution (3:1, H_2SO_4 : H_2O_2 by volume) for 20 minutes. This process caused vigorous oxidation. This was followed by two rinse cycles in deionized water ($18M\Omega cm^{-1}$). The coverslips were then dried using compressed air. The clean cover slips were coated with a 20nm layer of carbon using a Quoromtech QT150-TES Coater. The slides were then gradually heated in an oven to 300^0C. The slides were held at 300^0C for five minutes and then gradually cooled by reducing the temperature to 200^0C followed 150^0C, maintaining the temperature for five minutes in each case.

The deposited carbon layer provided a uniform heat absorption surface, to permit rapid local attainment of cavitation nucleation temperature. The cover slips were adhered to a glass cover slide with a film of deionized water in between as the cavitating medium. Parafilm was used as a spacer.

2.3. Temperature Measurement Setup

To enable estimation of the temperature at different distances from the bubble, a probe particle was trapped using the Ti:Sapphire laser while the fibre laser was used to produce a controlled bubble. Through the measurement of the probe particle position variance and knowledge of the size of the trapped particle and the trap stiffness, an estimation of the temperature at various distances from the bubble was acquired.

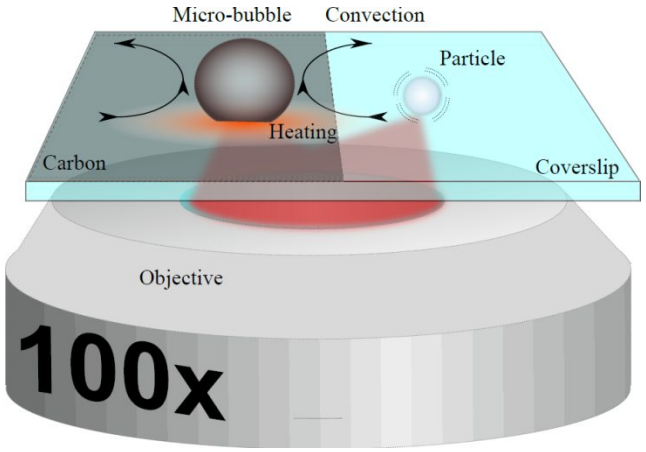

Fig. 2: Illustration of temperature measurement configuration**.** The half carbon coated coverslip that permits the simultaneous trapping of the probe particle (2.32µm silica) and the generation of controlled cavitation. Observed convection currents are illustrated.

In order to take this measurement a half carbon coated coverslip was required (Fig. 2), to prevent the generation of cavitation from the trapping laser, which would dislodge the particle from the trap. The half coated coverslips were fabricated in the same manner as described above, with a mask secured across half of the coverslip to prevent coating. A 2.32µm silica bead is used as the probe particle.

3. CONTROL SYSTEM

The control system implementation is based around the modulation of incident laser intensity using an SLM. Though use of other optical modulation techniques such as acousto-optic modulators or galvo mirrors would have increased the open loop bandwidth of the system the potential for simultaneous control of multiple bubbles offered through the modulation of multiple kinoforms was desirable for future investigations into microcavitation arrays and micromachinery actuation.

The radius of the induced cavitation bubble was manipulated through modulation of the kinoform phase. A noise mask of variable intensity was added to respective kinoform phases permitting the selective variation in laser spot intensity, illustrated in Fig. 3. Individual laser spot powers were thus controlled via the phase noise mask intensity.

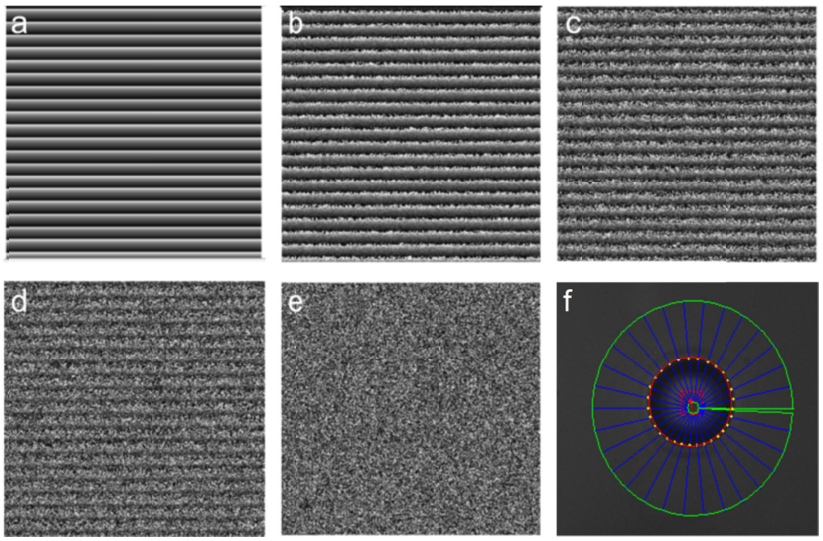

Fig. 3: An example of the kinoform noise mask modulation, applied to a single spot phase grating displayed on the SLM, (a) through (e)- noise intensities of 0%(a), 25%(b), 50%(c), 75%(d) and 100%(e) depict the reduction in prominence of the underlying phase grating. The noise mask intensity applied by the control algorithm varies continuously between 0 (0%) and 1 (100%). Note that the zero order spot is obstructed as full intensity modulation is only available for higher order laser spots. (f) Displays a graphical representation of the LabView (NI) machine vision algorithm used for circular edge detection. The concentric green circles designate the region of interest. The blue radial lines are examined for the highest pixel intensity gradient, and these areas are marked with white dots. Bilinear interpolation results in the red circle, a reasonable approximation for the bubbles dimensions.

Imaging of the slide was achieved using a a CCD camera (Prosilica GE680). Detection of the induced cavitation position and radius was facilitated via the NI LabVIEW Find Circular Edge detection algorithm (Fig. 3 (f)). This algorithm identifies the highest pixel intensity gradient along radial lines in a toroidal region of interest (ROI), and applies bilinear interpolation to determine the edge position. Circular fitting to the detected edge positions allowed estimation of the radius and circle centre position, provided the pixel output was calibrated to corresponding absolute measurements. Calibration was achieved through reference to a scaled calibration slide.

A Proportional Integral Derivative (PID) controller was implemented to provide feedback to the cavitation system, and facilitated the regulation of the cavitation radius. An error signal (t) , was calculated from the difference between the desired cavitation radius, $R(t)$, and the measured cavitation radius, $R_{measured}(t)$.

$$e(t) = R(t) - R_{measured}(t) \quad (1)$$

This error signal was converted into a control signal,$u(t)$, composed of a proportional error term, integral error term and derivative error term.

$$u(t) = K\left(T_p e(t) + \frac{1}{T_i}\int e(t)\,dt + T_d \frac{de(t)}{dt}\right) \quad (2)$$

Where the constants K(gain),T_P, T_i and T_d are tuneable parameters, to moderate the feedback damping and system stability. The control signal, $u(t)$, was added to a noise signal, $n(t)$, a floating point value with a

range between 0 and 1. This noise signal was multiplied by an array of randomly generated numbers, which was subsequently added to the phase of the hologram generating the respective spot. The control system is summarised in Fig. 4.

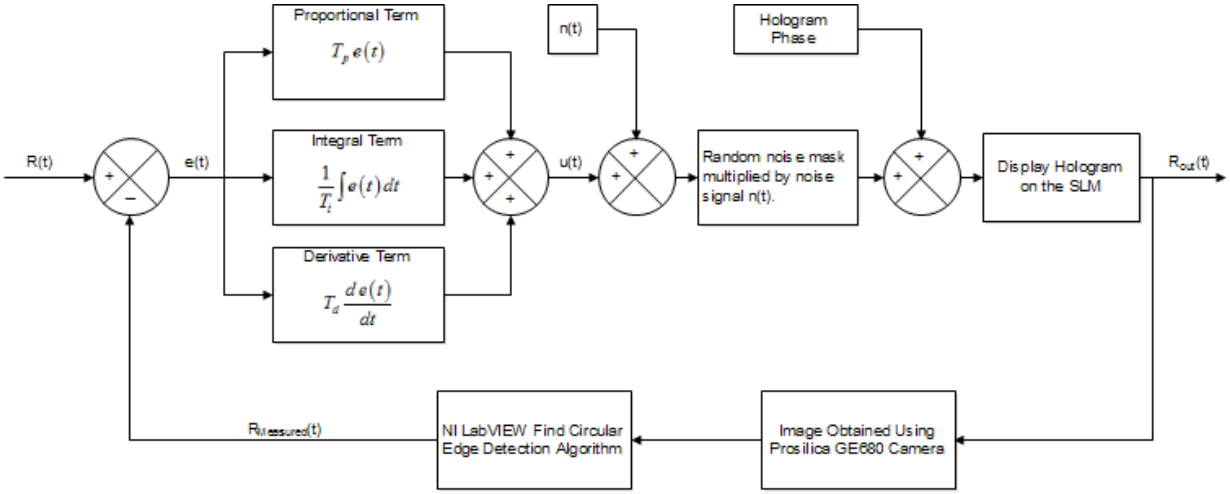

Fig. 4: The schematically representation of the Proportional Integral Derivative (PID) action developed for the microcavitation control. The difference between the specified desired radius, $\boldsymbol{R(t)}$, and the current measured radius, $\boldsymbol{R_{measured}(t)}$, is used to generate an error signal, $\boldsymbol{e(t)}$. This error signal is subsequently used to determine relevant proportional, integral and derivative feedback terms added to the noise signal, $\boldsymbol{n(t)}$, varying the kinoform phase noise and hence scattered light power for and individual laser spot.

4. PRECISE CONTROL OF LASER INDUCED CAVITATION

We aim here to demonstrate to what degree the cavitation process can be controlled and how the parameters of the system were varied to provide this type of control.

Successful independent control of individual microcavitation is evident in the step response output, as seen in Fig. 5 (a).
The results of the step response demonstrate the full control of cavitation radius between 5 and 8 microns. The output radius displays slightly underdamped dynamics, with a response that is akin to a second order oscillatory system.

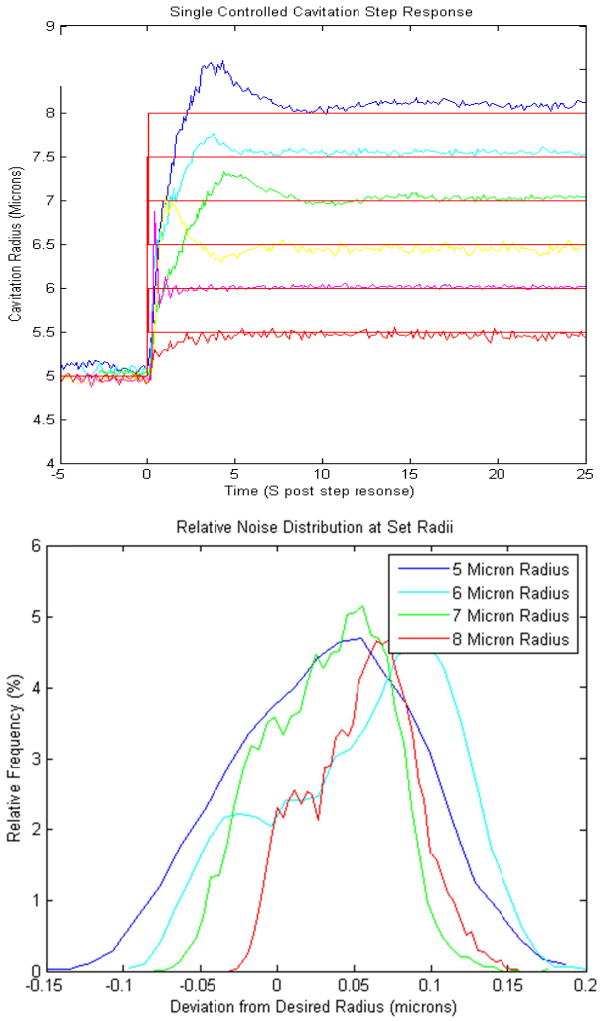

)

Fig. 5: (a) The radius change response of the controlled cavitation system is characterised in the step responses. The red plots represent the desired radii as input into the control system, and the coloured plots display the measured radii, as obtained from the NI LabVIEW Find Circular Edge detection algorithm. The general trend of increasing overshoot with increasing radius change signal indicates that the system is slightly underdamped. (b) The noise distribution of the measured radius about the desired radius is plotted for various radii at steady state. The positive bias indicates error in the integrator constant setting. Bimodal distributions in the higher order radii are indicative of periodic systematic error.

The positive bias in the noise distribution in Fig. 5 (b) is indicative of a minor error in the setting of the integrator constant, responsible for eliminating steady state error. Due to the relative sensitivity of this value in the given system of laser induced cavitation, it was difficult to reliably alter the steady state error on the order of tens of nanometers. The presence of a bimodal function in the output noise is suggestive of underlying periodic systematic error.

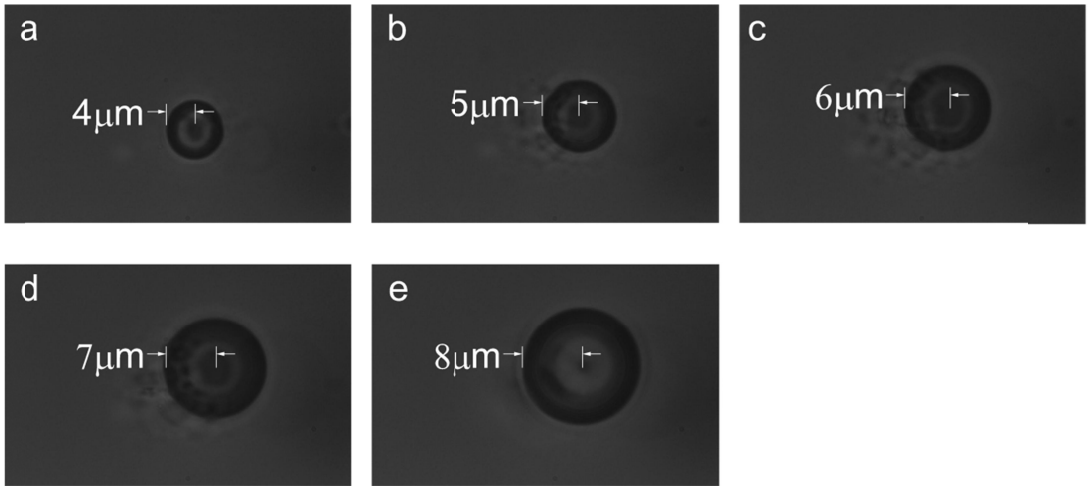

Fig. 6: Examples of controlled microcavitation at radii of 4(a), 5(b), 6(c), 7(d) and 8(e) micrometers. Note the particulate on the lower left side of the bubbles in (b), (c) and (d) was strongly attracted to the steady state cavitation.

When controlled microcavitation (Fig. 6) was initiated we observed a strong attraction of particles from within between 10 – 20 microns from the bubble surface. Such effects have been observed in previous studies and are explainable in terms of Marangoni convection currents [6]. Marangoni convection, or thermo-capillary convection is the temperature dependent mass transfer along the interface between two fluids due to surface tension gradient [6]. A possible application for the cavitation control achieved in this work would be as a platform for further investigation of Marangoni convection.

One of the key limitations in bubble control encountered was the focal region in which the edges of the bubble could be resolved with sufficient clarity for the edge detection algorithm to implement control. Manual adjustment of the focal length during larger changes in bubble radius (>3 μm) produced the best results in terms of stability and desired radius. Radius standard deviations on the order of 20nm were observed for steady state cavitation.

By applying a suitable kinoform which is able to produce multiple laser spots it is possible to generate an array of controlled microcavitation bubbles. This was, indeed, the primary justification for running laser intensity control via the SLM, as opposed to direct power modulation at the laser source. In the current experiment the maximum number of independently controlled cavitation generated using this setup was three (Fig. 7). However an approximately 0.5Hz oscillation with coupling between the three bubbles was observed for triad control. While this may be attributable to incorrect setting of relevant PID control parameters, it is suspected that this oscillatory output is the result of processing lag, as a drop in processed frame rate was also observed. For microcavitation arrays larger than three bubbles, streamlining of the control algorithm and additional system resources (than a quadcore desktop PC) are required.

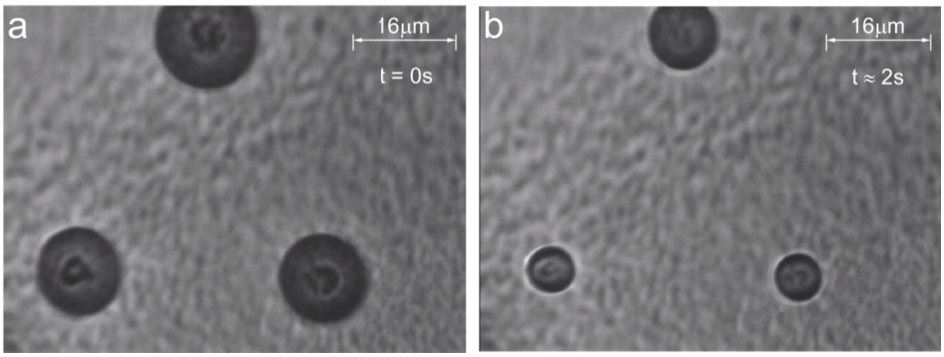

Fig. 7: Controlled Triad of bubbles. Frames (a) and (b) are separated by approximately 2s, and the coupled radius change is discernable. The radius setpoint was 7 microns during this trial.

5. TEMPERATURE MEASUREMENT AND REGULATION

.

An estimation of the temperature at various distances from the bubble was established through comparison with the trap stiffness. The trap stiffness was approximated as:

$$k = \frac{k_B T}{\left\langle \sigma^2 \right\rangle} \qquad (3)$$

Where k is the trap stiffness, k_B is Boltzmann's constant, T is the absolute temperature and $\left\langle \sigma^2 \right\rangle$ is the time averaged standard deviation of the probe particle position.

Given an appropriate calibration measurement of the trap stiffness, by trapping the probe particle in the absence of any cavitation and assuming the temperature of the slide can be approximated as ambient, the temperature at various distances from the cavitation may be estimated.

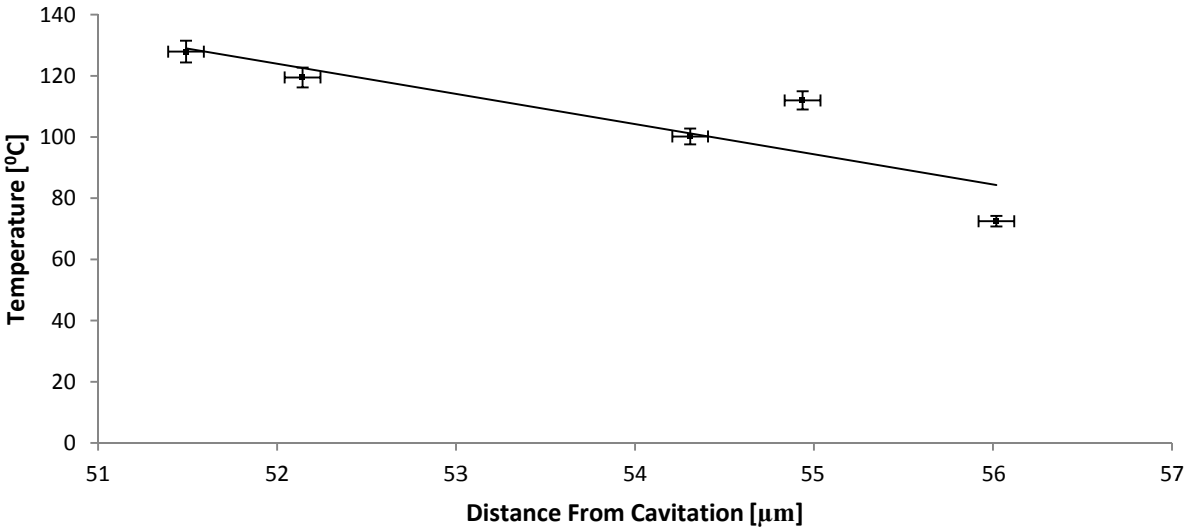

Fig. 8: Measured temperatures at various distances from a 4μm radius controlled microbubble. The acquired temperatures are based on the estimated trap stiffness which was measured through a separate calibration. The result at

54.9μm from the bubble is considered an outlier and is likely a result of insufficient lock in particle tracking or optical table disturbance, increasing the variance of this observation.

Temperature can be estimated in a simplified case of Marangoni convection, in which there is a linear temperature gradient at large distances, temperature distributions are unaffected by the flow and quadratic terms of the Navier-Stokes equation and can be neglected. In accordance with the work of Berry et al [6] , the temperature at a distance *r* from a bubble is approximated as:

$$T = T_0 + T_1\left(r + \frac{R^3}{2r^2}\right)\cos\theta \qquad (4)$$

Where T is the temperature at some distance, r, from the bubble, T_0 is the ambient temperature, T_1 is the temperature gradient at large distances from the bubble, and R is the radius of the bubble. The equation is expressed in spherical coordinates, accounting for the cosθ term.

A limitation of this experiment is the estimation of the calibration temperature. The assumption of the slide temperature being equivalent to ambient within close proximity to the trapping laser is inaccurate due to the associated heat flux. Hence the absolute temperature values evaluated in Fig. 8 do not necessarily represent the actual temperatures encountered. Nevertheless the results demonstrate linearity between temperature, variance and distance from a controlled microbubble, at distances on the order of 50 μm.

Due to the considerable convection currents encountered, temperature measurements at distances less than 50 microns are problematic as the probe particle tends to dislodge from the trap before sufficient position data can be collected. While the trapping laser power can be increased, unintentional generation of microcavitation and attraction of surrounding particles places limits on trapping laser power in practice. Better slide manufacturing will enable measurements closer to the microcavitation site.

6. CONCLUSION

The cavitation control methods presented demonstrate the viability of optical tweezers setups in the study of microbubble systems. The precision control established over both individual microbubbles and microbubble arrays permits both systematic study of cavitation and applications in microfluidics and optofluidically driven micromachines. The capacity for microcavitation to be used as a microscale temperature probe or regulator has also been demonstrated, with preliminary results on the temperature at various distances from controlled microcavitation site.

Future areas of investigation include experimental studies of Marangoni currents, perhaps involving the imaging of suitable tracer particles to categorise flow fields induced around cavitation in a controlled and repeatable manner. Such studies could be broadened to encompass the visualisation of flow fields generated by controlled microcavitation arrays facilitated through SLM control developed in this work. These systems will have potential microfluidic applications. Further streamlining of the control algorithm, hologram display and imaging techniques would facilitate the generation of more extensive microcavitation arrays. Due to the high precision of control, cavitation is an ideal candidate actuator for micromachinery or microfluidic devices requiring relatively large forces, in excess of those which conventionally are provided in optical trapping.

ACKNOWLEDGEMENTS

This work was supported by the Australian Research Council Discovery Grant (DP110103015). The authors would like to thank the Centre for Microscopy and Microanalysis, The University of Queensland for access to their facilities and training.

REFERENCES

[1] H. P. Le, "Additional Material, Journal of Imaging Science and Technology, Vol.51 No.2," *Imaging Science and Technology* **42**(5), 49–62 (1998).

[2] R. Dijkink and C.-D. Ohl, "Laser-induced cavitation based micropump.," *Lab on a chip* **8**(10), 1676–1681 (2008) [doi:10.1039/b806912c].

[3] Z. G. Li, K. Ando, J. Q. Yu, a Q. Liu, J. B. Zhang, and C. D. Ohl, "Fast on-demand droplet fusion using transient cavitation bubbles.," *Lab on a chip* **11**(11), 1879–1885 (2011) [doi:10.1039/c0lc00661k].

[4] S.-Y. Park, T.-H. Wu, Y. Chen, M. a Teitell, and P.-Y. Chiou, "High-speed droplet generation on demand driven by pulse laser-induced cavitation.," *Lab on a chip* **11**(6), 1010–1012 (2011) [doi:10.1039/c0lc00555j].

[5] D. Ahmed, C. Y. Chan, S.-C. S. Lin, H. S. Muddana, N. Nama, S. J. Benkovic, and T. Jun Huang, "Tunable, pulsatile chemical gradient generation via acoustically driven oscillating bubbles.," *Lab on a chip* **13**(3), 328–331 (2013) [doi:10.1039/c2lc40923b].

[6] D. W. Berry, N. R. Heckenberg, and H. Rubinsztein-Dunlop, "Effects associated with bubble formation in optical trapping," *Journal of Modern Optics*(September 2012), 37–41 (2009).

[7] D. Leszczynski, C. M. Pitsillides, R. K. Pastila, R. R. Anderson, P. Charles, R. Rox, and C. P. Lin, "Laser-Beam-Triggered Microcavitation : A Novel Method for Selective Cell Destruction Laser-Beam-Triggered Microcavitation : A Novel Method for Selective Cell Destruction," *Radiation Research* **156**(4), 399–407 (2001).

[8] V. P. Zharov, R. R. Letfullin, and E. N. Galitovskaya, "Microbubbles-overlapping mode for laser killing of cancer cells with absorbing nanoparticle clusters," *Journal of Physics D: Applied Physics* **38**(15), 2571–2581 (2005) [doi:10.1088/0022-3727/38/15/007].

[9] E. Zwaan and C. Ohl, "Sonoporation of suspension cells with a single cavitation bubble in a microfluidic confinement Se," *Lab on a chip*, 1666–1672 (2007) [doi:10.1039/b712897p].

[10] A. Salehi-reyhani, J. Kaplinsky, E. Burgin, M. Novakova, J. Andrew, R. H. Templer, P. Parker, M. A. A. Neil, O. Ces, et al., "Lab on a Chip PAPER A first step towards practical single cell proteomics : a microfluidic antibody capture chip with TIRF detection †," *Lab on a chip*, 1256–1261 (2011) [doi:10.1039/c0lc00613k].

[11] D. Preece, R. Bowman, A. Linnenberger, G. Gibson, S. Serati, and M. Padgett, "Increasing trap stiffness with position clamping in holographic optical tweezers.," *Optics express* **17**(25), 22718–22725 (2009).

[12] R. W. Bowman, G. Gibson, D. Carberry, L. Picco, M. Miles, and M. J. Padgett, "iTweezers: optical micromanipulation controlled by an Apple iPad," *Journal of Optics* **13**(4), 044002 (2011) [doi:10.1088/2040-8978/13/4/044002].

[13] R. Bowman, D. Preece, G. Gibson, and M. Padgett, "Stereoscopic particle tracking for 3D touch, vision and closed-loop control in optical tweezers," *Journal of Optics* **13**(4), 044003 (2011) [doi:10.1088/2040-8978/13/4/044003].